10-1-2008

Stochastic Event Reconstruction of Atmospheric Contaminant Dispersion Using Bayesian Inference

Inanc Senocak
Boise State University

Nicolas W. Hengartner
Los Alamos National Laboratory

Margaret B. Short
University of Alaska Fairbanks

W. Brent Daniel
Los Alamos National Laboratory

Stochastic Event Reconstruction of Atmospheric Contaminant Dispersion using Bayesian Inference

Inanc Senocak [a,*] Nicolas W. Hengartner [b] Margaret B. Short [c] W. Brent Daniel [b]

[a] *Boise State University, Department of Mechanical and Biomedical Engineering, Boise ID 83725*

[b] *Los Alamos National Laboratory, Los Alamos, NM 87545*

[c] *Department of Mathematics and Statistics, University of Alaska Fairbanks, Fairbanks, AK 99701*

Abstract

Environmental sensors have been deployed in various cities for early detection of contaminant releases into the atmosphere. Event reconstruction and improved dispersion modeling capabilities are needed to estimate the extent of contamination, which is required to implement effective strategies in emergency management. To this end, a stochastic event reconstruction capability that can process information from an environmental sensor network is developed. A probability model is proposed to take into account both zero and non-zero concentration measurements that can be available from a sensor network because of a sensor's specified limit of detection. The inference is based on the Bayesian paradigm with Markov chain Monte Carlo (MCMC) sampling. Fast-running Gaussian plume dispersion models are adopted as the forward model in the Bayesian inference approach to achieve rapid-response event reconstructions. The Gaussian plume model is substantially enhanced by introducing stochastic parameters in its turbulent diffusion parameterizations and estimating them within the Bayesian inference framework. Additionally, parameters of the likelihood function are estimated in a principled way using data and prior probabilities to avoid tuning in the overall method, The event reconstruction method is successfully validated for both real and synthetic dispersion problems, and posterior distributions of the model parameters are used to generate probabilistic plume envelopes with specified confidence levels to aid emergency decisions.

Key words: Bayesian Statistics, Event Reconstruction, Source Characterization, Gaussian Plume Models, Markov chain Monte Carlo (MCMC)

Preprint submitted to Atmospheric Environment *27 April 2008*

1 Introduction

Event reconstruction of chemical or biological (CB) agent dispersion into the atmosphere is an important *inverse problem* in homeland security and environmental monitoring applications. In event reconstruction, (also referred to as source characterization or source inversion in various studies) the major goal is to characterize the source of an atmospheric contaminant dispersion event in terms of release location and emission rate by using time-averaged concentrations and wind measurements that can be available from a sensor network. Event reconstruction tools can provide critical information for first-response and remediation efforts. Once the dispersion event is characterized in terms of modeling parameters, forward projections of the dispersion event can also be performed to quantify the extent of exposure to contamination.

Event reconstruction of atmospheric contaminant dispersion has received growing interest in recent years. Different methods have been adopted to address the problem. For instance, Thomson et al. (2007) applied an inverse problem approach to locating a known gas source from measurements of gas concentration and wind data. A search algorithm with a simulated annealing method was employed to find the source location and emission rate. Simulated annealing was found to be advantageous as it helps prevent the search algorithm from converging to local minima that might surround the targeted global minimum. In their study, three cost functions with different regularization terms were evaluated, and the cost function that minimizes the total source emissions was found to be the most robust, producing successful event reconstructions.

Allen et al. (2007a) developed a source characterization method in which a forward dispersion model was coupled with a backward receptor model using a genetic optimization algorithm. A puff model was used in the source characterization. The method was validated with both synthetic and experimental field data. Allen et al. (2007b) extended this method by considering the wind direction as an unknown parameter in addition to the source location and emission rate. A Gaussian plume model was considered instead of the puff model. The capability was only tested against synthetic concentration data with white noise. The results show that the method is capable of computing the correct solution, as long as the magnitude of white noise does not exceed the original concentration data.

Several recent event reconstruction studies have favored the Bayesian inference approach over the optimization approach as it offers several advantages (Johannesson et al., 2004; Chow et al., 2006; Keats et al., 2007). The main distinguishing feature of the Bayesian inference method is that it estimates

* Corresponding author.
Email address: senocak@boisestate.edu (Inanc Senocak).

probability distributions for parameters of interest and quantifies the uncertainty in the estimated parameter, whereas an optimization method provides point estimates for the parameters of interest through maximizing or minimizing an objective function.

Johannesson et al. (2004) presented dynamic Bayesian models using Monte Carlo methods for target tracking and atmospheric dispersion event reconstruction problems. Both the well established Markov chain Monte Carlo (MCMC) approach and the sequential Monte Carlo approach for dynamic problems are discussed in detail in their study. Chow et al. (2006) and Neumann et al. (2006) extended the Bayesian event reconstruction approach of Johannesson et al. (2004) to neighborhood scale atmospheric dispersion events. Both computationally intensive computational fluid dynamics (CFD) models, and computationally less intensive empirically based Gaussian puff models were adopted in these studies, respectively. The results of Chow et al. (2006) and Neumann et al. (2006) have shown that the Bayesian methodology is efficient in delivering probabilistic answers to the event reconstruction problem.

With high-fidelity models, the longer simulation times needed for event reconstructions can limit their applications in emergency response operations. Marzouk et al. (2007) reformulated the Bayesian approach to inverse problems by using polynomial chaos expansions to represent random variables. In their study a transient diffusion problem was considered. The results have shown that significant gains in computational time can be obtained by adopting the new scheme over direct sampling. Keats et al. (2007) considered a source-receptor relationship within the Bayesian inference method to reduce the overall computation time for source determination. An adjoint equation for the contaminant concentration was solved for that purpose. The method was tested for event reconstruction of dispersion within an array of obstacles, and for the Oklahoma city Joint Urban 2003 atmospheric dispersion study. The results show that the method can be considered successful in reconstructing the source location and the emission rate. The results also indicate that improving the forward model physics and incorporating the model uncertainty can be helpful in reducing the discrepancy between the model predictions and the experiment.

Indoor environments are also susceptible to dispersion events. Sreedharan et al. (2006) developed a systems approach for rapid detection of toxic agents in the indoor environment. A Bayesian interpretation approach is adopted to evaluate the effects of response time, threshold level, accuracy and overall performance of sensor systems. The method employs a two-stage Bayes Monte Carlo algorithm. In the first stage, a library of indoor dispersion simulations are created that cover probable release scenarios with varying airflow conditions. The creation of the simulation library can be computationally expensive, and it has to be prepared before a dispersion event. In the second stage, the observations

are assessed for their statistical agreement with simulations from the library, and the most likely situations are identified based on their probabilities.

Thus far, existing event reconstruction studies have mainly focused on characterizing the dispersion source in terms of its location and strength. In the case of a dispersion event, both zero and non-zero concentration readings can be available from a sensor network, and there is a need to incorporate all the sensor readings in a collective fashion. Furthermore, predictions can suffer from technical problems due to empirically defined constants that may appear in both the probability and the dispersion models. To the best of our knowledge, a detailed account of these issues has not been established within the context of event reconstruction problems. Hence, the primary objective of the present study is to address these specific issues in a principled way by exploiting the Bayesian inference framework.

In what follows, a stochastic event reconstruction method is presented, extending the Bayesian inference methodology described in Johannesson et al. (2004) and Chow et al. (2006). In particular, a probability model is introduced to take into account both zero and non-zero concentration measurements that can be available from a sensor network because of a sensor's specified limit of detection. Additionally, observed data and prior probability concepts are exploited to avoid arbitrary tuning of parameters in the probability model on a case by case basis. Fast-running Gaussian plume dispersion models have been employed in event reconstruction methods to satisfy the rapid emergency response requirements (Thomson et al., 2007; Allen et al., 2007b). Within the range of their applicability, a Gaussian plume model is also adopted in the present study, but its performance is uniquely enhanced by reformulating its empirical turbulent diffusion parameterizations with stochastic parameters. Finally, the event reconstruction method is successfully validated using both real and synthetic test cases, under spatially constant and variable wind conditions.

2 Bayesian Formulation

The forward modeling problem can be defined as predicting the response of a system using a physical theory (forward model) and system parameters. In the inverse modeling problem, an inference is made on the values of system parameters based on observations of the system response (Tarantola, 2005). Loosely speaking, inverse problems can be formulated as follows:

$$\mathbf{m} \approx F^{-1}(\mathbf{d}), \tag{1}$$

where $\mathbf{d}$ is a vector of observations, $\mathbf{m}$ is a vector of forward model parameters, and the operator F is the forward model that governs the system response. Inverse problems can be ill-conditioned, because small changes in $\mathbf{d}$ can lead to large changes in $\mathbf{m}$. The present event reconstruction problem requires estimating the model parameters $\mathbf{m}$ (e.g. release location, emission rate, wind direction etc.) given the observed concentrations $\mathbf{d}$ from a sensor network. Depending on the applications of inverse problems, both deterministic and probabilistic approaches have been developed for solving them (Vemuri, 2002). The probabilistic approach is pursued in the present study, and it is explained in the following.

Bayes' theorem defines the posterior probability density of a set of model parameters $\mathbf{m}$ given the observations $\mathbf{d}$ as follows (Gilks et al., 1996; Carlin and Louis, 1996).

$$p(\mathbf{m}|\mathbf{d}) = \frac{L(\mathbf{d}|\mathbf{m})p(\mathbf{m})}{p(\mathbf{d})}, \tag{2}$$

where $p(\mathbf{m}|\mathbf{d})$ is the *posterior probability density*, $L(\mathbf{d}|\mathbf{m})$ is the *likelihood function*, $p(\mathbf{m})$ is the *prior probability density*, and $p(\mathbf{d})$ is the *marginal probability density*. The posterior probability density given in Eq. (2) defines the conditional probability density of forward model parameters $\mathbf{m}$, given the observed data $\mathbf{d}$. Calculation of $p(\mathbf{m}|\mathbf{d})$ is central in Bayesian inference, and it can be seen as a solution to an inverse problem.

Direct computation of the posterior density, using Bayes' theorem, necessitates the computation of the marginal probability density given in Eq. (2). This can be computationally intensive to the point of being impractical for most applications. A practical approach for estimating properties of the posterior distribution is to perform MCMC sampling by noting the following (Metropolis et al., 1953; Carlin and Louis, 1996; Gilks et al., 1996)

$$p(\mathbf{m}|\mathbf{d}) \propto L(\mathbf{d}|\mathbf{m})p(\mathbf{m}). \tag{3}$$

Within this framework, the observed data $\mathbf{d}$ enters the Bayesian formulation only through the likelihood function.

In the present event reconstruction problem, specification of the likelihood function deserves attention, because it models how the concentration observations are acquired. For instance, sensors cannot reliably quantify the concentration of trace amounts of contaminants that may be at levels below the sensor's specified limit of detection. In that situation, a sensor may read a zero concentration value, ignoring the possible existence of trace amounts of contaminants. Treatment of zero sensor readings within the Bayesian framework is an issue. For instance, zero sensor readings can be discarded or represented as a negligibly small number. However, both approaches may lead to biased distributions. Alternatively, a probability model can be assumed for the existence of trace amounts of contaminants that may not be detected due to the

sensor's specified limit of detection. In other words, a likelihood function can be constructed in such a way that it accounts for zero sensor readings, when in fact the actual concentration can be non-zero.

Let $\mathbf{m}$ be the model parameters, C_m the predicted concentration, ξ_i the concentration measured by an ideal sensor i, and d_i the concentration observed by an actual sensor i. It is assumed that the observations d_i are related to ξ_i as follows:

$$d_i = \begin{cases} 0, \text{ with probability } \exp(-\alpha \cdot C_m) \\ \xi_i, \text{ with probability } 1 - \exp(-\alpha \cdot C_m) \end{cases} \tag{4}$$

and ξ_i, given the model, has a lognormal distribution with density

$$p(\xi_i|\mathbf{m}) = \frac{1}{\sqrt{2\pi}\sigma\xi_i} \cdot \exp\Big(-\frac{1}{2\sigma^2}(\log \xi_i - \log C_m)^2 \Big), \tag{5}$$

where σ^2 is the variance of the distribution. In Eq. (4), it is assumed that the probability of not detecting a plume can be calculated based on the predicted concentration C_m, and at the threshold concentration C_{th} the plume is detected with probability $1/2$, from which α can be computed as

$$1 - \exp(-\alpha \cdot C_{th}) = \frac{1}{2} \quad \Longrightarrow \quad \alpha = \frac{1}{C_{th}} \log(2). \tag{6}$$

Then, the likelihood function for a single datum d_i can be formulated as follows:

$$\begin{aligned} L(d_i|\mathbf{m}) &= \int_0^\infty p(d_i, \xi_i|\mathbf{m}) d\xi_i \\ &= \mathbb{I}[d_i = 0] \int_0^\infty \exp(-\alpha C_m) p(\xi_i|\mathbf{m}) d\xi_i + \\ &+ \mathbb{I}[d_i > 0] \int_0^\infty \left[1 - \exp(-\alpha C_m)\right] p(\xi_i|\mathbf{m}) \delta_{d_i}(\xi_i) d\xi_i, \end{aligned} \tag{7}$$

where δ_{d_i} is the Dirac delta-function. Therefore, the likelihood function can be written as:

$$\begin{aligned} L(d_i|\mathbf{m}) =& \mathbb{I}[d_i = 0] \cdot \exp(-\alpha C_m) + \\ &+ \mathbb{I}[d_i > 0] \frac{(1 - \exp(-\alpha C_m))}{\sqrt{2\pi}\sigma d_i} \cdot \exp\Big(-\frac{1}{2\sigma^2}(\log d_i - \log C_m)^2 \Big) \end{aligned} \tag{8}$$

It should be noted that the above likelihood function depends on the assumed probability of observing the data. Different likelihood functions can also be developed under different assumptions.

A forward model is needed to calculate the model concentration C_m. In emergency response situations, the overall run-time for delivering answers is an important factor. Hence, fast running Gaussian plume dispersion models are

adopted as the *forward model*. A Gaussian plume dispersion model for uniform steady wind conditions can be written as follows (Panofsky and Dutton, 1984):

$$C_m(x,y,z) = \frac{Q}{2\pi U\sigma_y\sigma_z}\cdot\exp\left(-\frac{y^2}{2\sigma_y^2}\right)\cdot \\ \cdot\left\{\exp\left(-\frac{(z-H)^2}{2\sigma_z^2}\right)+\exp\left(-\frac{(z+H)^2}{2\sigma_z^2}\right)\right\}, \tag{9}$$

where $C_m(x,y,z)$ is the concentration at a particular location, Q is the emission rate or the source strength, U is the mean wind speed and H is the height of the release. Here, x is the distance along the wind, y is the distance along the horizontal crosswind direction, and z is the distance along the vertical axis. Note that the release location is the origin for x, y and z directions. In the above equation σ_y and σ_z are the standard deviation in the horizontal crosswind and vertical directions, respectively. These two parameters are also known as the Gaussian plume dispersion parameters, and they are defined empirically for different stability conditions. For Pasquill C type stability, Briggs formulas for urban conditions parameterize the standard deviations as follows (Panofsky and Dutton, 1984):

$$\sigma_y = 0.22\cdot x\cdot(1+0.0004\cdot x)^{-0.5}, \quad \sigma_z = 0.20\cdot x. \tag{10}$$

Several problem-specific formulas have been proposed for σ_y and σ_z. Results typically benefit from adjusting these empirical parameters for different problems. In the present study, the empirical constants 0.22 and 0.20 in Eq. (10) are replaced with stochastic parameters ζ_1 and ζ_2, respectively. The following is written for the turbulent diffusion parameterizations

$$\sigma_y = \zeta_1\cdot x\cdot(1+0.0004\cdot x)^{-0.5}, \quad \sigma_z = \zeta_2\cdot x. \tag{11}$$

As shown in the next section, the event reconstruction results are significantly improved by adopting this approach. It is emphasized that the above concept is not specific to the Gaussian plume model, but it can be applied to the empirical parameters of other dispersion models.

The probability model is completed by specifying prior distributions for the model parameters $\mathbf{m} = (x, y, Q, H, \theta, U, \zeta_1, \zeta_2, \sigma^2)$. In Eq. (3), $p(\mathbf{m})$ represents prior knowledge or ignorance about the model parameters ($\mathbf{m}$) before observing the data $\mathbf{d}$. Within the Bayesian framework, this can be expressed by specifying prior distributions that place bounds on the model parameters, based on known physical properties or expert opinion. For instance, data regarding the probability of certain wind directions and magnitudes acting on a city might be available from previous meteorological studies.

For the error variance σ^2, which represents measurement and model errors in a cumulative fashion with a lognormal distribution, an inverse gamma prior

distribution is assumed (Carlin and Louis, 1996),

$$p(\sigma^2|\alpha,\beta) = \frac{1}{\Gamma(\alpha)\beta^{\alpha}}(\sigma^2)^{-(\alpha+1)}\exp(-1/(\beta\sigma^2)). \tag{12}$$

The hyperparameters α=1.0 and β=1000.0 specify a vague yet proper prior distribution.

For the model parameters $x, y, U, H, \theta, \zeta_1, \zeta_2$, proper uniform priors are assigned. In each case, the parameters are constrained to lie in a domain which is bounded by practical values (Sivia, 1996). The emission rate, Q, is associated with the magnitude of the dispersion event. Hence, a *Jeffrey's prior* is preferred (Sivia, 1996), and the following can be written

$$p(Q) = \mathbb{I}[Q > Q_{min}]\,/Q, \tag{13}$$

where Q_{min} is a practical lower limit for the emission rate. It should be noted that specifying a prior distribution is subjective, and different prior distributions can be suggested.

Given the the prior distributions for $\mathbf{m}$ and the likelihood function as shown in Eq. 8, the posterior distribution for $\mathbf{m}$ given the data can be written as

$$p(\mathbf{m}|\mathbf{d}) \propto \{\prod_{i=1}^{N} L(d_i|\mathbf{m})\} \times p(\mathbf{m}), \tag{14}$$

where N is the total number of sensors in the network, and i is the sensor identification number. It is understood that

$$p(\mathbf{m}) = p(x)p(y)p(Q)p(H)p(U)p(\theta)p(\zeta_1)p(\zeta_2)p(\sigma^2). \tag{15}$$

Note that, conditional on the model $\mathbf{m}$, it is assumed that observations are independent, and that a priori, the model parameters that comprise $\mathbf{m}$ are also independent.

Various algorithms exist for MCMC sampling. In the present study, the Metropolis algorithm is adopted to simulate samples from the posterior distributions (Metropolis et al., 1953). The reader is referred to Gilks et al. (1996) and Carlin and Louis (1996) for a detailed explanation of the algorithm. In the Metropolis algorithm, a candidate state $\mathbf{m}^*$ is sampled from a Gaussian distribution centered on the previous state $\mathbf{m}$, and the candidate state is accepted with probability

$$\rho(\mathbf{m}, \mathbf{m}^*) = \min\left(\frac{\pi(\mathbf{m}^*)}{\pi(\mathbf{m})}, 1\right). \tag{16}$$

where the target distribution is defined as

$$\pi(\mathbf{m}) = L(\mathbf{d}|\mathbf{m}) \cdot p(\mathbf{m}). \tag{17}$$

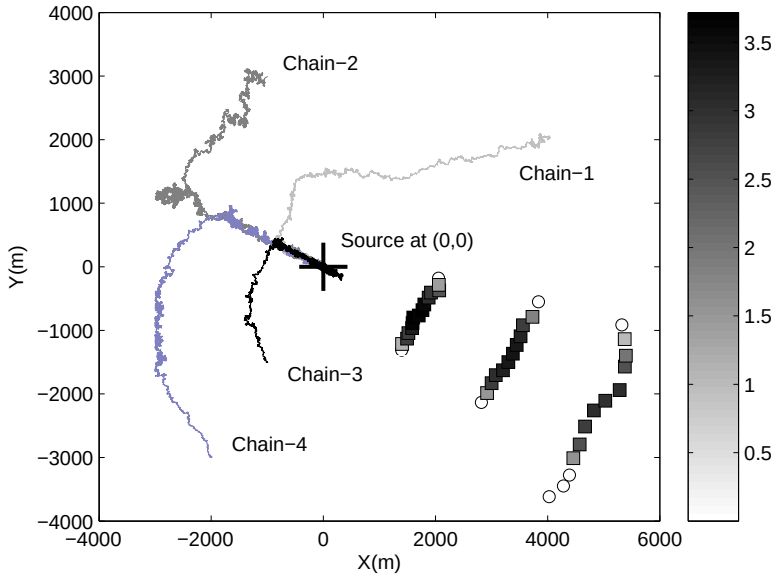

Fig. 1. Traces of four independent Markov chains. The true value of the SF6 release location is also marked. Square markers denote sampler/sensor locations colored with measured concentration levels in ng/m^3. Logarithmic (base 10) values are shown. Clear circular markers indicate sensors measuring zero concentration.

Note that the proposals ($\mathbf{m}^*$) are made sequentially for each model parameter in the practical implementation.

3 Results

Environmental sensor networks have been deployed in various cities, and specifics of these networks and actual data from the sensor network are not publicly available. Hence, direct testing of event reconstruction methods against such data are not feasible. Tracer field experiments designed for atmospheric dispersion and air pollution studies can be used to evaluate the performance of event reconstruction models (Bradley et al., 2005). Similarly, for problems where the conditions are highly variable and field experiments are not feasible, synthetic data can be produced by adding random error to forward simulation results. Both approaches are pursued to validate the present event reconstruction model.

3.1 Event Reconstruction of Copenhagen Tracer Experiments

A series of tracer experiments were performed in the Copenhagen area in 1978 and 1979. Concentrations of tracer sulphurhexafluoride (SF6) and meteorolog-

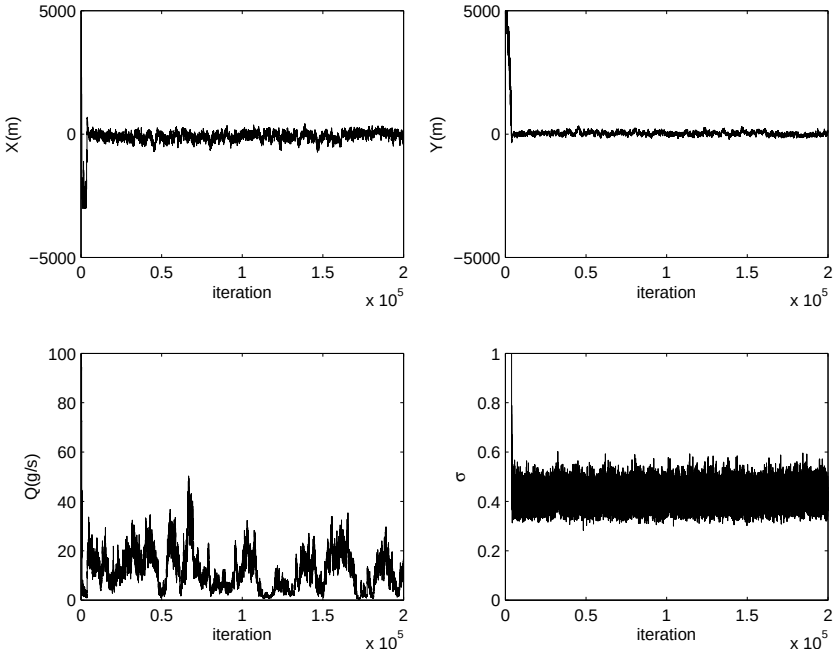

Fig. 2. Convergence of model parameters x, y, Q and σ with MCMC iterations.

ical conditions were measured and reported in Erik and Lyck (2002). For all the experiments, the SF6 tracer was released from a tower with a height of 115 m. Samplers/sensors were placed $2-3$ m above the ground level along three crosswind arcs that were positioned $2-6$ km away from the tracer release point. The total sampling time for the concentration measurements was one hour. In the tracer data corresponding to the experiment performed on October 19, the detection limit was given as 9 ng/m^3, and any value below this limit was indicated as zero. This value is used to set the sensor threshold value C_{th} in Eq. (6) of the stochastic event reconstruction method. Out of the forty samplers, eight of them register zero concentration values, as indicated in Fig. 1 with clear markers. In the present study, the tracer dispersion experiment is reconstructed for nine model parameters $(x, y, H, Q, \theta, U, \zeta_1, \zeta_2, \sigma^2)$. Fig. 1 shows traces of Markov chains starting from four different locations. The samplers are are colored with one hour averaged concentration measurements reported in (Erik and Lyck, 2002). Fig. 1 shows that, after an initial "burn-in" period, the MCMC chains generate samples from the vicinity of the true source location independent of their starting points.

To assess the present event reconstruction method, a single simulation with a long Markov chain was performed. The simulation with 2×10^5 MCMC iterations took 143 s to finish on a laptop with Intel Core2 Duo (T7200) 2.0 GHz processor. The code used only a single processor core during the simulation. Fig. 2 shows the convergence plots of model parameters x, y, Q and σ. The first 20% of the chain is discarded as the burn-in period, and the remaining samples are used in analyzing the posterior distributions. Similar convergence behavior is also observed for the remaining model parameters.

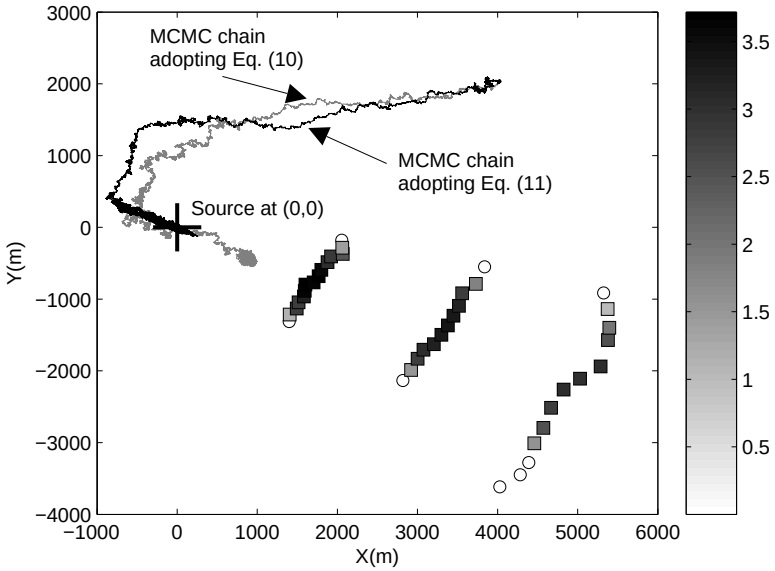

Fig. 3. Impact of adopting stochastic parameters in the forward model. Clear circular markers indicate sensors measuring zero concentration.

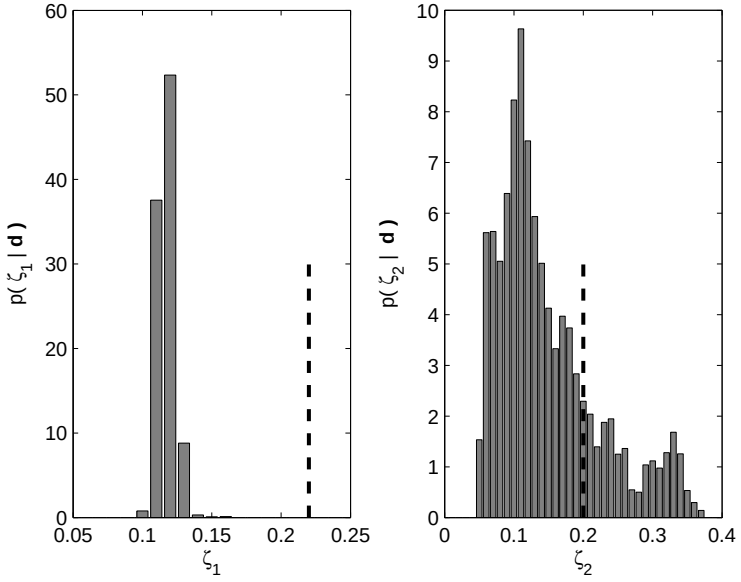

Fig. 4. Marginal probability distribution of stochastic turbulent diffusion parameters given in Eq. (11). The vertical dashed lines highlight constant empirical values given in Eq. (10).

The original Gaussian plume model is modified in this study by introducing stochastic parameters in the empirical turbulent diffusion parameterizations (e.g. Eq. (11)). As shown in Fig. 3, event reconstruction of the release location is substantially improved when turbulent diffusion parameters are estimated stochastically as opposed to empirically defining them in Eq. (10), which re-

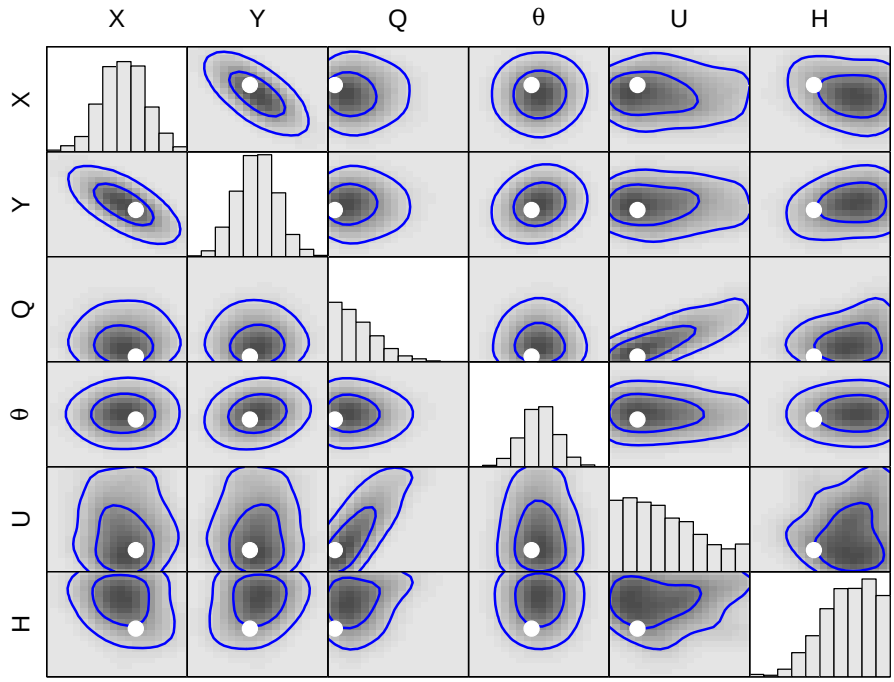

Fig. 5. Bivariate posterior distributions of event reconstruction parameters. The diagonal plots present marginal distributions. The white marker represents true values from the field experiment of Erik and Lyck (2002). The outer and inner contour lines envelopes 90% and 50% of the samples, respectively.

sulted in posterior draws concentrated in an area that is roughly 1000 m away from the true source location.

Fig. 4 shows the posterior distributions of the stochastic parameters given in Eq. (11). The constant parameters given in Eq. (10) are also indicated on this plot. The posterior distribution of the stochastic term ζ_1 suggest values that are markedly different than the value given in Briggs formulas. It is also observed that the results are more sensitive to σ_y formulation, as the posterior distribution indicates a narrow band for the stochastic parameter ζ_1, and the empirical value suggested in the Briggs formula does not lie within the high posterior probability region of ζ_1. An obvious advantage of the present approach is that posterior distributions of the forward model parameters can be used in post-event forward projection calculations to get improved estimates of contamination extent.

In typical emergency response operations, one of the primary goals is to find the location of the release. Probabilistic answers instead of deterministic answers are naturally preferred by decision makers due to many uncertainties involved in CB agent dispersion events. To address this need, posterior distri-

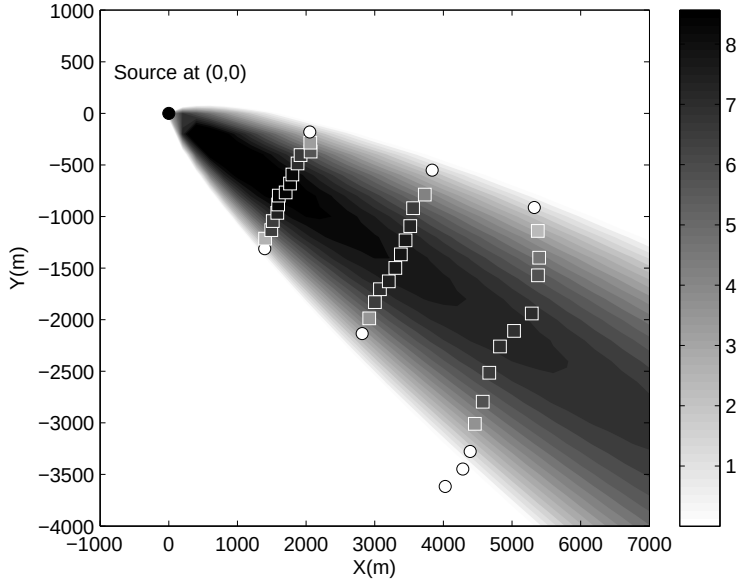

Fig. 6. Probabilistic plume envelope for 95% confidence level. Concentration unit is ng/m3 and logarithmic values are plotted. Clear circular markers indicate sensors measuring zero concentration.

butions need to be mapped in terms of probabilities. Because several parameters can be inferred in event reconstruction problems, a careful check using bivariate analysis is needed. For that purpose, the results are summarized on a so-called trellis plot as shown in Fig. 5. The plots on the diagonal are marginal probability distributions of the forward model parameters. The off diagonal plots are joint posterior distributions of the forward model parameters. The outer and inner contour lines enveloping 90% and 50% of the samples are also overlaid on the joint posterior distributions. The results from the field experiment are highlighted with white colored markers on each subplot, which are successfully captured within high posterior probability regions.

In atmospheric dispersion events, it is important that emergency responders are provided with results that can address the uncertainty involved in the problem. Bayesian inference approach was shown to be convenient for that purpose (Chow et al., 2006). Fig. 6 presents a probabilistic plume envelope with a confidence level of 95%. The plume envelope is generated by running a forward model for each posterior sample and storing the concentrations on a vector at desired locations. Then, the concentration value corresponding to the 95^{th} percentile in the data is selected as the probabilistic plume envelope. As can be seen from Fig. 6, the plume envelopes all the samplers/sensors. Hence, in analyzing this plot, one can have 95% confidence in assuming that actual concentration could be any value that is below the value read from the probabilistic plume envelope. Fig. 7 provides a check of this assumption. Concentration data from the probabilistic plume envelope is compared against

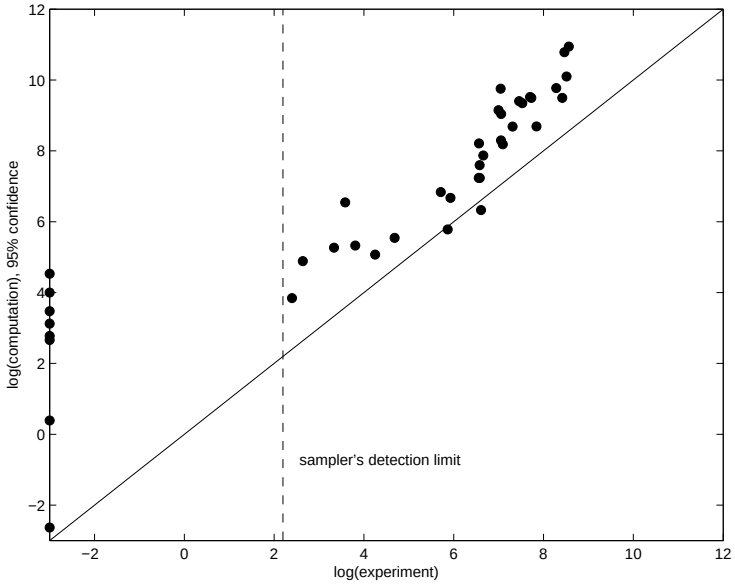

Fig. 7. Scatter plot comparison of concentration values obtained from the probabilistic plume envelope with 95% confidence level vs. concentrations measured at each sensor.

the actual concentration measurements from the samplers on a scatter plot. As expected, 95% of the data are over predicted by the simulation; this results in more conservative (safer) decisions in case of harmful dispersion events.

3.2 Event Reconstruction of a Synthetic Dispersion Experiment with Spatially Varying Winds

Meteorological conditions over an urban area can be highly variable with winds and stability conditions changing throughout the day. Hence, event reconstruction models should also have capabilities to address dispersion events under such conditions. Various physical models exist to model spatially varying winds and contaminant dispersion. These models can range from simple fast-running empirical models to high-fidelity CFD-based models that demands large resources for computation. In the present study, a fast-running segmented Gaussian plume dispersion model is adopted, in which the overall plume is divided into segment. Each segment is then calculated using the straight-line Gaussian plume model driven by the local wind conditions. For a detailed explanation of the segmented Gaussian plume, the reader is referred to Burger and Mulholland (1988). It should be emphasized that Gaussian plume models have been developed under certain assumptions (Panofsky and Dutton, 1984), They may not perform well for complex urban dispersion problems, in which the original modeling assumptions are not satisfied. In such cases, advanced high-fidelity dispersion models may perform better than the Gaussian plume models.

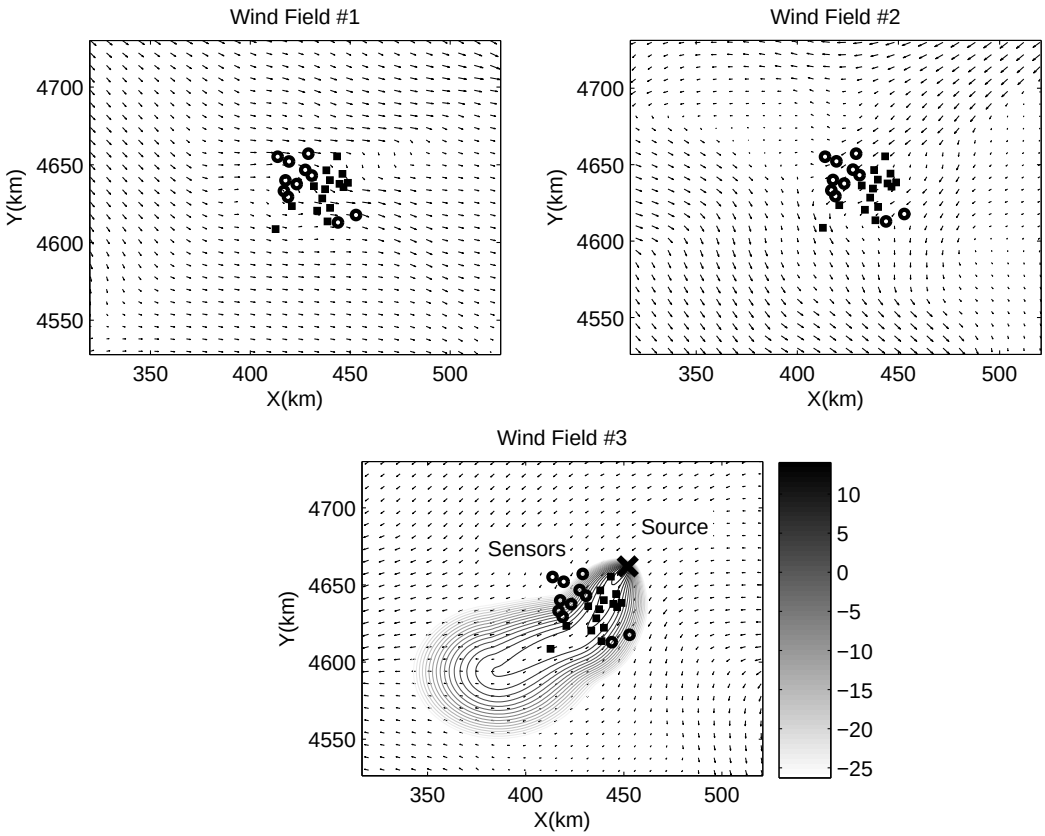

Fig. 8. Approximate wind fields generated from scattered wind measurements, using the Barnes objective analysis scheme (Koch et al., 1983). Each vector plot represent synthetic mean wind fields at different times in the day. Synthetic plume dispersion is driven by the third wind field. Circular markers indicate sensors with zero synthetic concentration readings. Non-zero synthetic concentration readings are represented with square markers

Wind field information over an area of interest can be available in terms of wind measurements from scattered locations at different times of the day. Various data assimilation techniques have been developed to extend wind field measurements onto a regular grid. In the present study, the practical Barnes Objective analysis scheme (Koch et al., 1983) is used to extrapolate wind fields on a two-dimensional gridded domain, which is then used to drive the segmented Gaussian plume model for dispersion calculations. It should be noted that the accuracy of the wind interpolation approach is not critical for the present problem because data are treated as synthetic truth. However, advanced data assimilation and high fidelity numerical weather prediction models can be employed in actual operations.

Fig. 8 show three wind fields obtained by interpolating time-averaged wind field measurements at scattered locations. Each interpolated wind field is assumed to be representative of conditions during a certain time interval. Measurements are assumed to have been made at equally spaced time intervals.

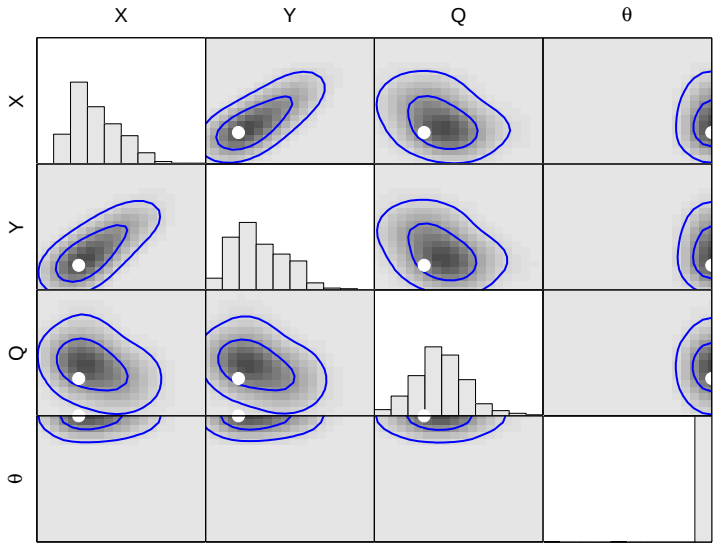

Fig. 9. Bivariate posterior distributions of event reconstruction parameters. The diagonal plots present marginal distributions. The white marker represents true values from the synthetic experiment. The outer and inner contour lines envelope 90% and 50% of the samples, respectively.

To set up the *synthetic* dispersion event problem, the segmented plume model was run on the third wind field as shown in Fig. 8. Gaussian noise with zero mean and a standard deviation that is 10% of the synthetic sensor's assumed limit of detection is added to the logarithm of model concentrations to mimic actual sensor observations with a lognormal error distribution. The x and y coordinates of the release location, the emission rate Q and the wind field identification number θ (e.g. $\theta = 1, 2, 3$) and error variance σ^2 are estimated in the synthetic event reconstruction problem.

Fig. 9 shows a bivariate analysis of the event reconstruction results. As can be seen from this figure, the true values from the synthetic experiment lie within the contour line that envelopes 50% of the samples. In analyzing the posterior distributions for the wind field identification number θ, one can notice that the third wind field has the highest posterior probability. This is not surprising because slight variations in the wind field can lead to drastic changes in the dispersion patterns and poor agreements with the observed concentrations.

As described in the Bayesian formulation section, the present study adopts a likelihood function to takes into account zero concentration sensor readings. Fig. 10 demonstrates the benefits of the present approach. As can be seen from this figure, the simulation that discarded the zero sensor readings points to a most probable source location that is roughly 20 km away from the synthetic true answer. However, when the zero sensor readings are taken into account,

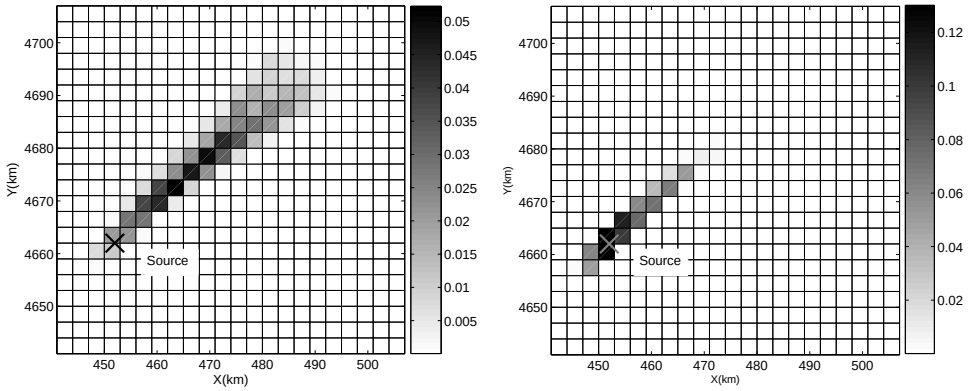

Fig. 10. The impact of zero sensor treatment on the event reconstruction results. The plot on the left shows a simulation in which zero sensor readings are discarded. The plot on the right shows a simulation that retains zero sensor readings using Eq. (8). The mesh is color-coded by probability.

the synthetic true answer lies within a region of high posterior probability. This shows the importance of retaining the zero sensors and modeling them within the Bayesian framework.

4 Conclusion

A stochastic event reconstruction method for atmospheric contaminant dispersion has been presented. The method is based on Bayesian inference with MCMC sampling. Special attention was given to the formulation of the likelihood function to take into account both zero and non-zero concentration measurements that can be available from a sensor network. Additionally, parameters in the likelihood function are treated as random, and they are estimated by using both data and prior probabilities to avoid arbitrary tuning in the overall method. Fast-running Gaussian plume dispersion models have been adopted as the forward model in the Bayesian framework. The Gaussian plume model has been uniquely enhanced by reformulating its empirical turbulent diffusion parameterizations with stochastic parameters that are estimated in the Bayesian inference framework.

The event reconstruction method has been successfully validated against real and synthetic dispersion experiments. In particular, the modeling of zero sensors and the stochastic estimation of turbulent diffusion parameters have substantially improved the results. In practice, release location and emission rates are of great importance to the emergency responders. The present study has shown that the event reconstruction problem can be posed with several parameters. In the event reconstruction of the Copenhagen tracer experiment, up to

nine parameters were estimated. Posterior probability distributions of model parameters were also used to generate probabilistic plume envelopes with specified confidence levels that can be useful in constructing hazard zones to aid emergency decision makers.

Although the Bayesian inference framework is general, a comprehensive operational event reconstruction tool needs to address various release scenarios. The present study focused on steady-point source releases. However, possible contaminant release scenarios may include line, area or moving sources. Furthermore, the scale of the event may range from neighborhood scale to urban scale, requiring different dispersion models at each scale. A Gaussian plume model may not be suitable at the neighborhood scale, where the impact of individual buildings on dispersion patterns are significant. In such cases, advanced dispersion models should be considered. Future work will concentrate on adding new dispersion capabilities to the present stochastic event reconstruction tool (SERT) to address these various release scenarios.

Acknowledgements

This work was supported by the LDRD funds of the Los Alamos National Laboratory. The authors wish to thank Michael Williams and Michael Brown for helpful discussions.

References

Allen, C. T., Haupt, S. E., Young, G. S., 2007a. Source characterization with a genetic algorithm-coupled dispersion-backward model incorporating SCIPUFF. Journal Applied Meteorology 41, 465–479.

Allen, C. T., Young, G. S., Haupt, S. E., 2007b. Improving pollutant source characterization by better estimating wind direction with a genetic algorithm. Atmospheric Environment 41, 2283–2289.

Bradley, M. M., Kosovic, B., Nasstrom, J. S., 2005. Models and measurements: Complementary tools for predicting atmospheric dispersion and assessing the consequences of nuclear and radiological emergencies. Lawrence Livermore National Laboratory, UCRL-PROC-216924.

Burger, L. W., Mulholland, M., 1988. Real-time prediction of point-source distributions using an anemometer-bivane and a microprocessor. Atmospheric Environment 22, 1309–1317.

Carlin, B. P., Louis, T. A., 1996. Bayes and Empirical Bayes Methods for Data Analysis. Chapman and Hall.

Chow, F. K., Kosovic, B., Chan, S. T., 2006. Source inversion for contaminant

plume dispersion in urban environments using building-resolving simulations. In: 6th Symposium on the Urban Environment, American Meteorological Society.

Erik, S., Lyck, E., 2002. The Copenhagen tracer experiments: Reporting of measurements. Riso National Laboratory, Riso-R-1054(rev.1)(EN).

Gelman, A., Carlin, J. B., Stern, H. S., Rubin, D. B., 2003. Bayesian Data Analysis. CRC Press.

Gilks, W. R., Richardson, S., Spiegelhalter, D. J., 1996. Markov Chain Monte Carlo in Practice. Chapman and Hall.

Hogan, W. R., 2006. Atmospheric dispersion modeling in biosurveillance. In: Wagner, M. M., Moore, A. W., Aryel, R. M. (Eds.), Handbook of Biosurveillance. Academic Press.

Johannesson, G., Hanley, B., Nitao, J., 2004. Dynamic Bayesian models via Monte Carlo-An introduction with examples. Lawrence Livermore National Laboratory, UCRL-TR-207173.

Keats, A., Yee, E., Lien, F., 2007. Bayesian inference for source determination with applications to a complex urban environment. Atmospheric Environment 41, 465–479.

Koch, S. E., desJardins, M., Kocin, P. J., 1983. An interactive Barnes objective map analysis scheme for use with satellite and conventional data. Journal of Climate and Applied Meteorology 22, 1487–1503.

Marzouk, Y. M., Najm, H. N., Rahn, L. A., 2007. Stochastic spectral methods for efficient Bayesian solution of inverse problems. Journal of Computational Physics 224, 560–586.

Metropolis, N., Rosenbluth, A. W., Rosenbluth, M. N., Teller, E., 1953. Equation of state calculations by fast computing machines. Journal of Chemical Physics 21, 1087–1092.

Neumann, S., Glascoe, L., Kosovic, B., Dyer, K., Hanley, W., Nitao, J., 2006. Event reconstruction for atmospheric releases employing urban puff model UDM with stochastic inversion methodology. In: 6th Symposium on the Urban Environment, American Meteorological Society.

Panofsky, H. A., Dutton, J. A., 1984. Atmospheric Turbulence. John Wiley.

Sivia, D. S., 1996. Data Analysis, A Bayesian Tutorial. Oxford Uiversity Press.

Sreedharan, P., Sohn, M. D., Nazaroff, A. J. G. W. W., 2006. Systems approach to evaluating sensor characteristics for real-time monitoring of high-risk indoor. Atmospheric Environment 40, 3490–3502.

Tarantola, A., 2005. Inverse Problem Theory and Methods for Model Parameter Estimation. SIAM, Philadelphia.

Thomson, L. C., Hirst, B., Gibson, G., Gillespie, S., Jonathan, P., Skeldon, K. D., Padgett, M. J., 2007. An improved algorithm for locating a gas source using inverse methods. Atmospheric Environment 41, 1128–1134.

Vemuri, V., 2002. Inverse problems. In: Bekey, G. A., Kogan, B. Y. (Eds.), Modeling and simulation: Theory and Practice, A Memorial Volume for Prof. Walter J. Karplus. Kluwer Academic Publishers, Boston.